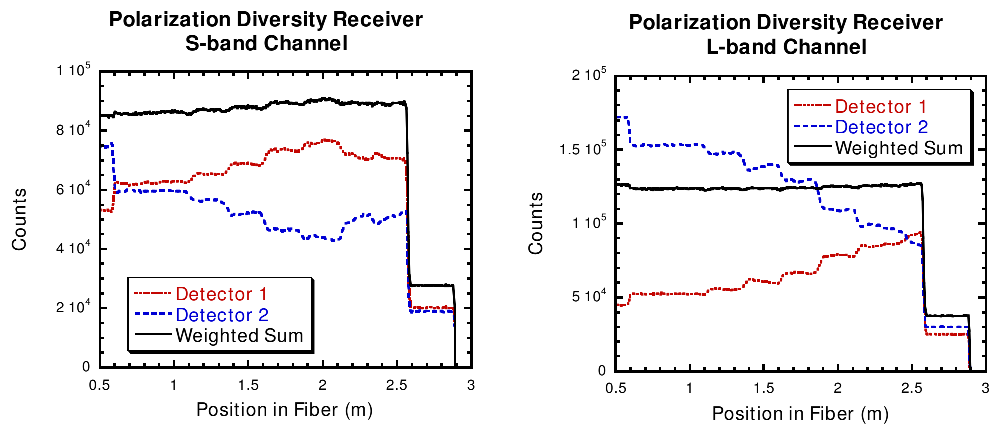

(a) (b)

Fig. 6. Plots of measured histogram data obtained with a polarization diversity receiver, showing the raw histogram data for the "H" and "V" polarizations, as well as the weighted sum of the two polarizations. Note that the weighted sum data are much more smooth (less fluctuations created by fiber bends) than the raw histograms for the two polarizations. (a) Histograms from the S-band channel (1460 – 1490 nm). (b) Histograms from the L-band channel (1570 – 1610 nm).

To calculate the temperature of the fiber under test, we first calculated a weighted sum of the histograms from the two polarizations. The weighting factor is determined by the ratio of the detection efficiency (DE) of the two SNSPDs used to record the histograms for the "H" and "V" polarization states. The weighted-sum histograms are also shown in Fig. 6, and it is clear that the weighted-sum histograms are significantly less sensitive to the bend-induced polarization effects than the raw histograms from of the two polarizations.

From the weighted histogram data for the S-band and L-band channels, we then calculate the temperature of the fiber by use of Eq. (5) above. The resultant temperature as a function of position in the fiber is shown in Fig. 7. Also in Fig. 7 is a plot of the fiber temperature versus position when the polarization diversity receiver is not used (measurement system shown in Fig. 1 was used instead). In this figure we have indicated the approximate locations of the fiber meander bends. The data were taken at room temperature, so we expect a flat temperature profile. The PDR has significantly reduced the undesired fluctuations in the temperature versus position in the fiber. However, the temperature result of the PDR example still exhibits unwanted fluctuations. The higher-frequency fluctuations are likely noise-induced, as described in the uncertainty analysis, and could be reduced with higher pump power or longer integration periods. The lower-frequency fluctuations are more likely the result of residual polarization effects. We hypothesize that these fluctuations might result from the fact that we did not have four SNSPDs available for this experiment, so there was a short delay (a few minutes) and a change of fiber connections between the measurements of S-band and L-band channels, which might result in some residual polarization fluctuations.

7. Conclusions

We have demonstrated a distributed fiber-optic temperature sensor with extremely high spatial resolution, as a result of the unique properties of our SNSPDs. The low timing jitter of the SNSPDs (on the order of 65 ps) enables spatial resolution on the order of 1 cm. Early demonstrations of distributed temperature sensors used multimode fiber to increase the collection efficiency of the Raman scattered photons, but here we are able to demonstrate a sensing system with standard telecom single-mode optical fiber. We expect that our technique could be applied to extremely long-range distributed sensors, because it is compatible with low-loss single-mode fiber and therefore unaffected by multimode fiber dispersion. Previously, we detailed the modifications necessary to achieve range on the order of 1 km while maintaining the low temperature uncertainty and high spatial resolution [7].

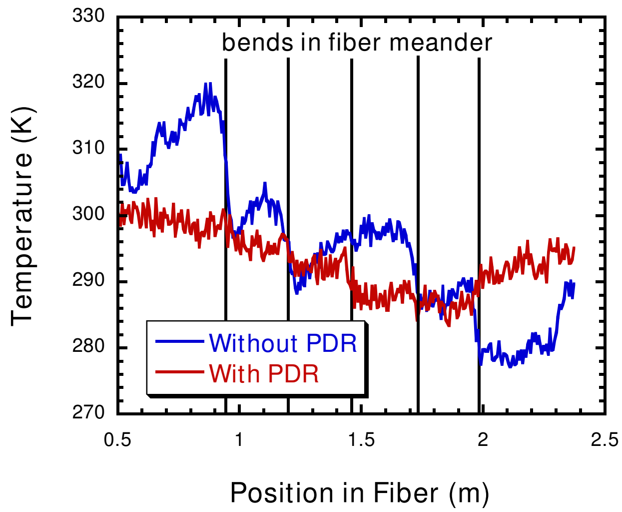

Fig. 7. Plot of measured temperature versus position in the sensing fiber. The sample was the two-dimensional fiber meander described above. For this particular measurement, the entire system was held at room temperature. Measurement was performed both with and without a polarization diversity receiver (PDR).

Our measurement system is capable of achieving extremely low temperature uncertainties: on the order of 3 K for a measurement integration period of 1 minute. The temperature uncertainty is currently limited by statistical fluctuations and it can be improved by increasing the integration period. Improvements in the temperature uncertainty are also possible with higher pump power, lower loss filters and/or higher efficiency SNSPDs. Alternatively, the temperature uncertainty can be improved by performing spatial averaging of existing data, sacrificing spatial resolution for reduced uncertainty in temperature. For example, with the data in Fig. 4, temperature uncertainty of the order of 1 K can be achieved with a spatial resolution of 5 cm.

We have shown that this measurement is also affected by systematic uncertainties, such as the polarization variations in the backscattered light. We demonstrated improved measurement performance with a polarization diversity receiver. This measurement could potentially be applied as a primary thermometer, but a full characterization of the properties of the laser, filters, detectors, as well as a detailed characterization of all of the systematic uncertainties would be necessary.

Acknowledgments

The authors are grateful to the National Institute of Information and Communications Technology (NICT) of Japan for providing SNSPDs for this experiment. MGT and RHH acknowledge funding from the UK Engineering and Physical Sciences Research Council. RHH also acknowledges a Royal Society University Research Fellowship. The authors thank Robert Maier and Bill MacPherson for useful discussions.